Geopersia 2024, 14(2): 307-325
DOI: 10.22059/GEOPE.2024.373882.648749

RESEARCH PAPER

Some chemical variations in biotite, phlogopite, and muscovite, considering their tectonic setting

Nasser Ashrafi [1,*], Rahim Dabiri [2], Ahmad Jahangiri [3]

[1] Department of Geology, Payame Noor University, P.O. Box 19395-4697 Tehran, Iran
[2] Department of Geology, Mashhad Branch, Islamic Azad University, Mashhad, Iran
[3] Department of Earth Sciences, University of Tabriz, Tabriz, Iran

Received: 12 March 2024, Revised: 21 April 2024, Accepted: 11 May 2024

Abstract
Several studies have been conducted to investigate the composition of micas (especially biotite) with the magmatic suites of the host rock (especially granitoid), thus to understand the tectonic environment of the host rock. This study deals with the issue of what compositional trends or elemental correlations exist in igneous micas when a large dataset with a given tectonic environment is used. In this regard, variations in the chemical composition of biotite, phlogopite, and muscovite from intra-plate, rift, and arc environments were investigated, regardless of the composition of their host rock. Enrichment of Fe or Mg in micas, such as Mg-rich biotite or Fe-rich phlogopite, can make us wrong in determining whether a mineral is primary or secondary based solely on chemical composition. The negative and good correlation between FeO and MgO caused biotites and phlogopites of all three tectonic environments to follow the trend of the calc-alkaline orogenic suites of Abdel-Rahman's classification. Considering the excellent and negative correlation between Al and Mg in muscovite, the substitution of $2Mg^{2+} = 3Al^{3+}$ is significant in this mineral. The data distribution shows that biotites and phlogopites belonging to rift and convergent environments can be divided into Al-rich and Al-poor groups or Mg-rich and Mg-poor groups.

Keywords: Biotite, Phlogopite, Tectonic Setting, Mineral Chemistry.

Introduction

Micas, especially biotite, and phlogopite, are common ferromagnesian minerals in many volcanic, plutonic, and metamorphic rocks from different tectonic environments. They, as a whole, show considerable variation in chemical and physical properties (Deer et al., 2013), but all are characterized by the general formula of $I_2M_{4\text{-}6}T_8O_{20}(OH, F)_4$, where *I* is mainly K, Na or Ca but also Ba, Rb, Cs; *M* is mainly Al, Mg or Fe but also Mn, Cr, Ti, Li; and *T* is mainly Si or Al and possibly also Fe^{3+} and Ti (Rieder et al., 1998). The chemical composition of magmatic micas is sensitive to chemical and physical factors associated with the crystallization of the magma and can provide petrogenetic information (e.g., Heinrich, 1946; Foster, 1960; Wones & Eugster, 1965; Nachit et al., 1985; Munoz, 1992). The chemical composition of biotites is typically used to appraise the conditions in which their magmatic host rock were generated (Nachit et al., 2005; Samadi et al., 2021): oxygen fugacity (fO_2) in the parent magmas, liquidus temperature (T), to classify the granitoid (I- and S-type) as well as to date the thermal events registered by these rocks. Biotites cover a range of compositions from Mg-rich (phlogopite) to Fe-rich (annite, siderophyllite). The X_{FeO*} = FeO*/(FeO* + MgO) of biotites depends on that of the host rock; it

* Corresponding author e-mail: n_ashrafi@pnu.ac.ir

varies from $X_{FeO*} \approx 1$ in felsic rocks to $X_{FeO*} \approx 0$ in basic ones (Abrecht & Hewitt, 1988). Biotite has received much attention as a valuable indicator of relative fugacities of HF and HCl in hydrothermal fluids, since the distribution of F and Cl between granitic magmas and magmatic-hydrothermal fluids strongly affects metal ratio, the order of crystallization, the timing of vapour saturation, and mass transport in the magmatic-hydrothermal fluids and hydrothermal ore deposition (e.g., Munoz, 1984; Van Middelaar & Keith, 1990; Boomeri et al., 2006). Considering that biotite is abundant in the porphyry copper deposits (PCDs), extensive studies have been conducted on the determination of halogen contents in it with the aim of to identify mineralized and barren plutons (Ayati et al., 2008; Boomeri et al., 2009; Afshooni et al., 2013; Zhang et al., 2016; Moshefi et al., 2020; Feng et al., 2021). Biotites with high Mg/Fe ratios tend to incorporate more F, while low Mg/Fe ones contain more Cl, as noted by Munoz (1984). This correlation is caused by the crystal-chemical effect known as 'F-Fe avoidance" and "Mg-Cl avoidance" (Munoz, 1984). The solubility of Ti in Mg-biotite strictly depends on temperature and pressure. Empirical geo-thermometer dealing with Ti solubility in the Fe-Mg biotites has frequently been used to determine magmatic-hydrothermal temperatures in PCDs.

The major elements of biotite have been widely used for identifying the tectonic setting of igneous rocks (e.g., Abdel-Rahman, 1994). The study of the composition of biotite from various igneous rock types showed that biotites in alkaline anorogenic suites are mainly Fe-rich, biotites in peraluminous (including S-type) suites are siderophyllitic in composition, and those in calc-alkaline, mainly subduction-related orogenic suites are enriched in Mg (Abdel-Rahman, 1994). The most fractionated members of calc-alkaline magmas might become slightly to moderately peraluminous (Stussi & Cuney, 1996). However, it is well-established that the origin of most peraluminous granites is known to be different from that of calc-alkaline magmas. The Al vs. Mg diagram is used to relate the mica composition in granitoid to the nature of their parental magmas. In this regard, the parental magmas are classified into peraluminous, calc-alkaline, subalkaline, or alkaline/peralkaline (Nachit et al., 1985). Abdel-Rahman (1994) proposed MgO vs. Al_2O_3 and FeO vs. Al_2O_3 bivariate plots to discriminate between biotite from alkaline (anorogenic), calc-alkaline (orogenic), and peraluminous granitoid. Using a machine learning approach, Saha et al. (2021) showed that the rift settings biotite can be discriminated by low Mn, Mg, and high Ba, Ca. Oxygen fugacity is low in rift setting compared to the other tectonic settings (Cottrell et al., 2020), and the magmas tend to be reduced with high Fe/Mg. Such magmas evolve by early fractional crystallization of olivine and/or clinopyroxene leaving the residual magmas depleted in MnO (Foley et al., 2013; Mullen, 1983), which is probably the cause of the low Mn content in biotite from this setting (Barbarin, 1990). Meanwhile, higher concentrations of Mn, Na, and Ti and lower concentrations of Al, and Ba have the most substantial effect on the discrimination biotite in oceanic intra-plate rocks (Saha et al., 2021). Ocean island magmas tend to have lower Si and high Ti concentrations amongst all the tectonic settings. A deep melting source for the magmas is consistent with the high Ti and low Al of the biotites as Ti concentration of the melt increases while that of Al decreases with increasing pressure (Ueki & Iwamori, 2014). Low values of Na, Al, Cr, Ca, and Cl and high values of Mg, K are critical indicators of biotite from continental intra-plate tectonic settings. Continental intra-plate magmas are enriched in incompatible elements like K, Ba (Kovalenko et al., 2007) which might allow the incorporation of K, Ba into biotite during crystallization. Due to the presence of a thick continental lithosphere, ascending magmas may interact with mantle peridotite consuming olivine and crystallizing pyroxene and/or garnet. This melt-rock interaction can produce Mg-rich, Al-poor magma with high K_2O/Na_2O (Liu et al., 2017), which may explain the high Mg, K, and lower Na, Al of biotite that crystallizes from continental intra-plate magmas. Continental crust assimilation can also play an important role in enhancing the K_2O/Na_2O ratio of the magmas in such settings (Saha et al., 2021). In contrast, high Na, Ba, Al, F, and Cl, and low K and Mn apply significant control in discriminating biotite from continental

arc rocks. Such a chemical characteristic of continental arc biotite may reflect the contribution of slab components in the form of slab-derived melt and slab-derived fluid (Schmidt & Jagoutz, 2017; Huang et al., 2019). Nevertheless, some studies have questioned the utility of biotite chemistry in discriminating the tectono-magmatic setting of its host rocks (Shabani et al., 2003). Applying mica composition as a tracer of geological conditions requires a perfect description of the host rock features. For example, biotite is the most critical reservoir of any excess aluminium in granites that do not have essential amounts of garnet, cordierite, or the Al_2SiO_5 polymorphs; therefore, it directly reflects the peraluminosity of the host magma in such rocks (Shabani et al., 2003). Furthermore, it is critical to be sure that the biotite grains analyzed are of primary magmatic origin because the possible alteration by late- or post-magmatic fluids may modify the original composition inherited from mineral-melt equilibrium (Stussi & Cuney, 1996). In this regard, re-equilibrated and neo-formed biotite grains, resulting from low-temperature hydrothermal alteration, have less Ti than those of primary magmatic biotites (Patiño Douce, 1993; Stussi & Cuney, 1996; Nachit et al., 2005).

Among the questions about the use of micas for tectono-magmatic interpretations of the host rock, the following can be mentioned: In general, is there a link between the composition of biotite and the tectonic environment regardless of its host rock? Is the chemical composition of phlogopite, Mg-rich species of biotite, able to show the tectonic environment of its host rock or not? When relatively large mineral chemistry data are available, based on the major elements of micas, what are the dominant elemental trends and correlations in different tectonic environments? The present study answers the mentioned questions. To achieve this purpose, the mica dataset was adapted from the GEOROC database (http://georoc.mpch-mainz.gwdg.de/georoc). In this study, the major oxides of biotite, phlogopite and muscovite minerals from host rocks with a given tectonic environment, including arc, intra-plate or rift-related, were plotted in the conventional binary and ternary diagrams.

Materials and Methods

In this work, first of all, the dataset of electron probe micro-analyzer (more than 44000 analyses) of different mica minerals (including annite, biotite, celadonite, glauconite, hydro-mica, hydro-muscovite, lepidolite, margarite, muscovite, paragonite, phengite, phengite-muscovite, phlogopite, siderophyllite, yangzhumingite, and zinnwaldite) taken from the GEOROC, was examined. Since the three micas, biotite, phlogopite, and muscovite, are ubiquitous in igneous rocks, they were selected for the study. Among these data, ~34000 analyses of the minerals "biotite" (n=16365), "phlogopite" (n=12311), "muscovite" (n=1173), and "Mica" (n=3880) were selected because of having a complete series of their major element oxides. It should be noted that "Mica" group includes a combination of different types of mica minerals. Compositionally, the host rocks vary mainly from intrusive to volcanic types, covering a wide compositional range from ultramafic/mafic to felsic. Tectonically, the host rocks mainly belong to three critical tectonic settings, including intra-plate (n=22238), arc (n=5019), and rift-related (n=3660). The complete dataset, including citations, geographic locations, host rock types, tectonic settings, and mica type, is presented in the supplementary Table. Mineral formula calculations were done based on 22 atoms of oxygen and the presentation of the data used the GCDkit 6.1 program (Janousek et al., 2006).

Discussion

In the common micas, muscovite, phlogopite, and biotite, there appears to be no ordering of the different cation species, (Fe, Mg) in octahedral and (Si, Al) in tetrahedral sites, but in some other micas, distinct site preferences do occur (Deer et al., 2013). This feature can be seen in

the classification diagram of the International Mineralogical Association (IMA), where most of the biotite and phlogopite data plot close to the siderophyllite-eastonite boundary (Rieder et al., 1998) with a variable Mg/(Fe + Mg) ratio (Figure 1).

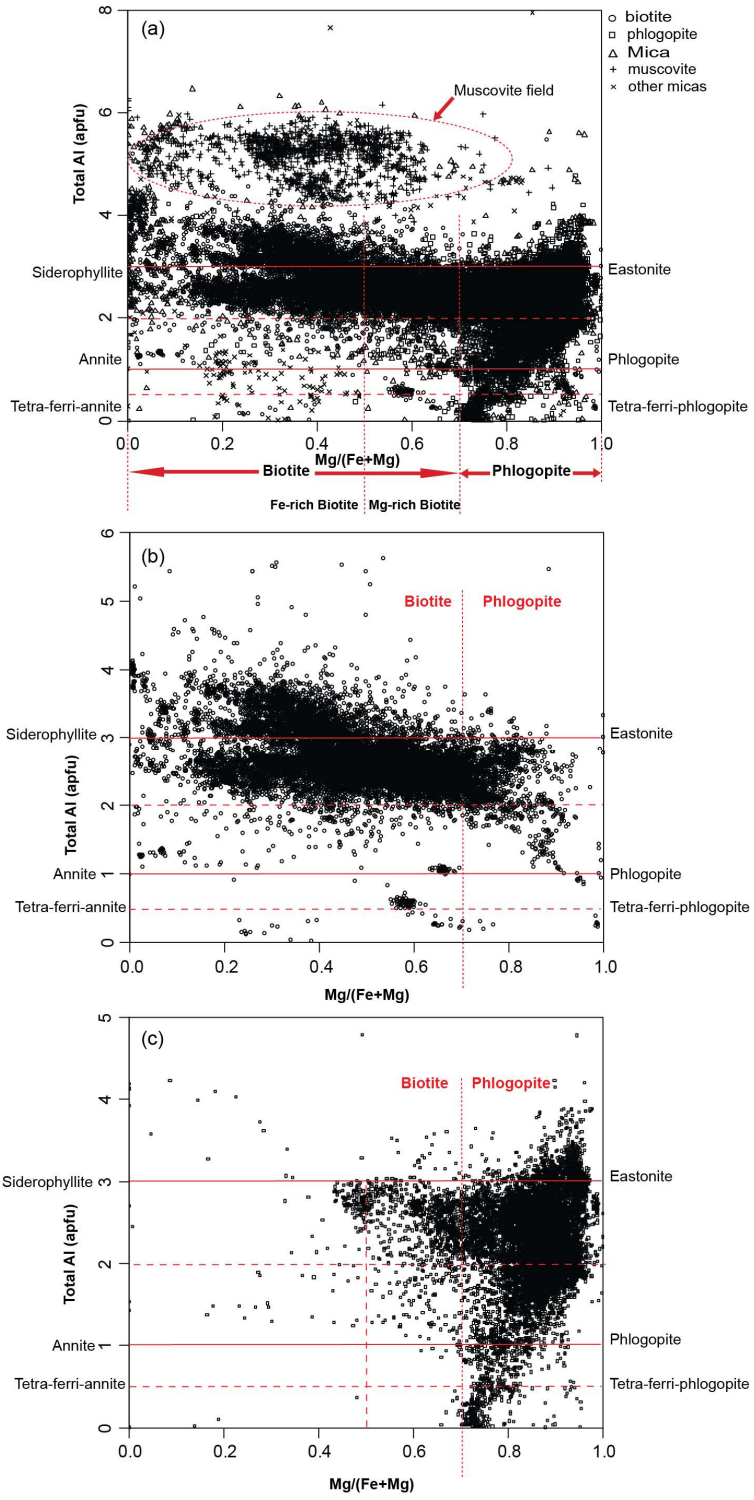

Figure 1. (a) Chemical composition of the whole dataset on the Mg/(Fe+Mg) versus Al^{tot} classification diagram of Rieder et al. (1998); biotite with Mg/(Fe+Mg)< 0.7 and phlogopite with Mg/(Fe+Mg)> 0.7 are distinguished; the dashed ellipse shows the approximate composition range of muscovite; (b) the plot of the biotite data; (c) the plot of the phlogopite data

In Figure 1a, the muscovite data are characterized by high amounts of Al^{tot} (4-6 atoms per formula unit, apfu), although they have variable Mg/(Fe + Mg) ratio like the biotite-phlogopite series (Figure 1b). This diagram also shows that when the Mg/(Fe+Mg)> 0.7, the variation of Al^{tot} in phlogopite is widespread (Figure 1c).

The ternary diagram TiO_2-(FeO^t + MnO)-MgO, proposed by Nachit et al. (2005), is a quantitative objective tool for distinguishing primary magmatic biotites from more or less re-equilibrated and neo-formed biotites. The limit of the domains of the primary magmatic biotites, the re-equilibrated biotites, and the neo-formed biotites were determined based on optical, paragenetic, and chemical criteria. Nevertheless, here we merely used this diagram to examine the variations in the chemical composition of micas from definite tectonic environments. In addition, we have used the conventional binary (Mg-Al^{tot}, MgO-FeO^t, MgO-Al_2O_3, FeO^t-Al_2O_3) and ternary (FeO^t-MgO-Al_2O_3) diagrams to investigate the major element changes of micas. Below, the biotite, phlogopite, Mica, and muscovite compositions from the given environments of convergent, intra-plate, and rift are plotted on the mentioned diagrams, and the similarities and differences of the trends are examined regardless of host rock type.

Most of the biotites from the host rocks with convergent setting plot in or around the primary biotite domain (Figure 2a) but phlogopite compositions do not follow this trend and they are plotted alongside MgO-TiO_2 (Figure 2b). Regarding the data that are not known to be "phlogopite", "biotite" or "muscovite", i.e., under the mineral title "Mica" in the dataset, they show a significant scattering (Figure 2c). If we plot the muscovite data in the ternary diagram, they will lie along the TiO_2-(FeO^t+MnO) side (Figure 2d).

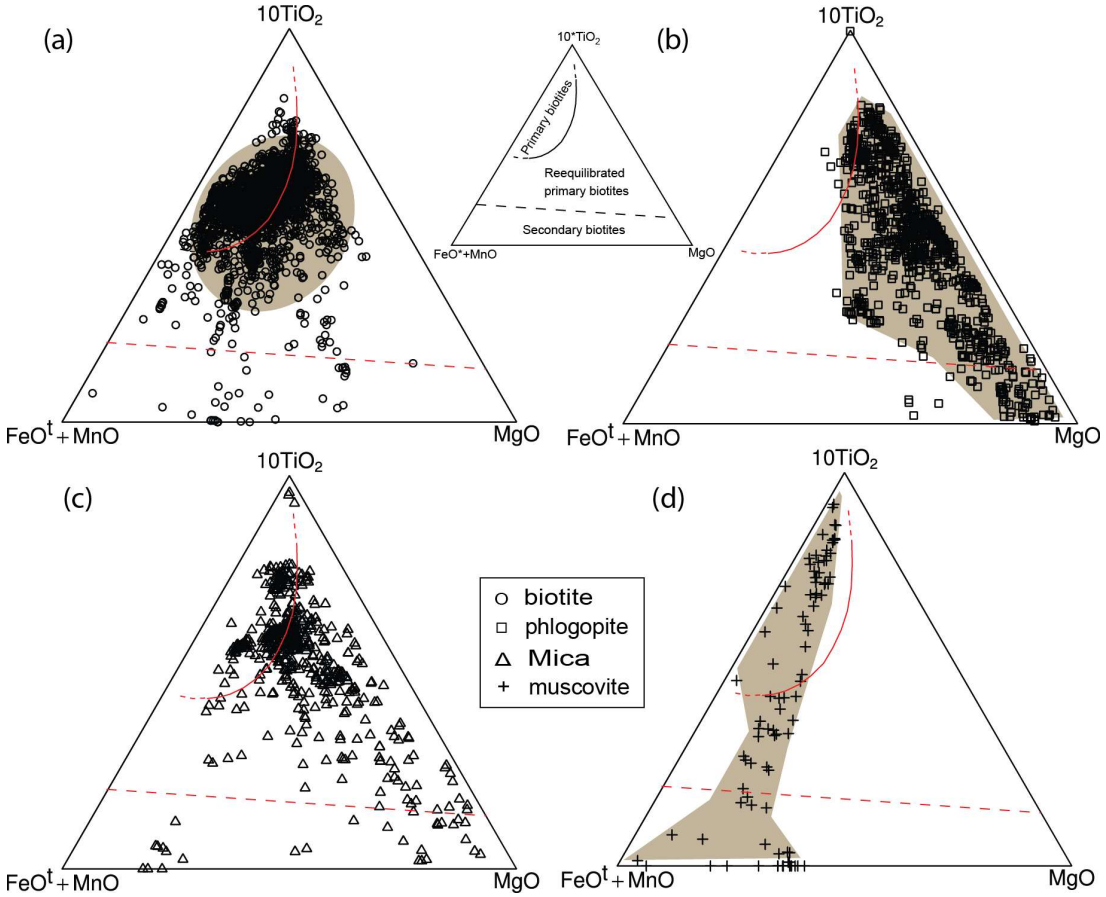

Figure 2. Ternary TiO_2–FeO+MnO–MgO diagram after Nachit et al. (2005); composition of biotite (a), phlogopite (b), Mica (c), and muscovite (d) from host-rocks of convergent setting. See the text for more details. FeO^t and FeO^*: total iron

Therefore, the data with non-biotite composition can give misleading results regarding their primary or secondary nature, and petrographic and paragenesis evidence must be included in confirming the final results.

The mentioned trends are almost similar for the intra-plate and rift settings (Figures 3a-d and 4a, c). However, the phlogopite data from the rift environment can be divided into two groups (Figure 4b), while the muscovite data are plotted in the middle of the triangle (Figure 4d).

Based on the study of Abdel-Rahman (1994), biotites in calc-alkaline granite suites, mostly subduction-related orogenic suites, are enriched in Mg. Investigations show that the biotites in orogenic alkaline suites (subduction-related foid-syenite and alkali-gabbro) also follow this trend (e.g., Ashrafi et al., 2009; the calc-alkaline field of Figures 5a-d). These trends seem to point to some elemental substitutions in the biotites (e.g., Fe^{2+}=Mg^{2+}; M^{2+} Si^{4+}= ^{M}Al ^{T}Al). Therefore, using the biotite composition of granitoid for the host magma suites or the geo-tectonic reconstruction of ancient orogens can be misleading (Stussi & Cuney, 1996).

The FeO^{t} vs. Al_2O_3 variation plot shows that the biotites of convergent setting can be divided into two groups (Figure 6a), while the phlogopites show a relatively concentrated distribution (Figure 6b). Also, these diagrams show that micas related to anorogenic alkaline suites are not very abundant (Figures 6a-c). There is no significant elemental correlation between FeO^{t} and Al_2O_3 in the first three diagrams (Figures 6a-c). Nevertheless, a good negative correlation can be seen in the muscovite data (Figure 6d).

According to the FeO^{t} vs. Al_2O_3 variation plot, the biotite and Mica compositions in the rift setting do not correlate (Figures 7a, d). In contrast, the phlogopite ones show a relatively negative correlation (Figure 7b). As to muscovite, an excellent negative correlation occurs at higher Al content (Figure 7d). These trends can be related to element substitutions $^{M}Fe^{2+}$ ^{T}Si=^{M}Al ^{T}Al, $^{M}Fe^{2+}$ $2^{T}Al$= $2^{T}Si$, and $3^{M}Fe^{2+}$=$2^{T}Al$.

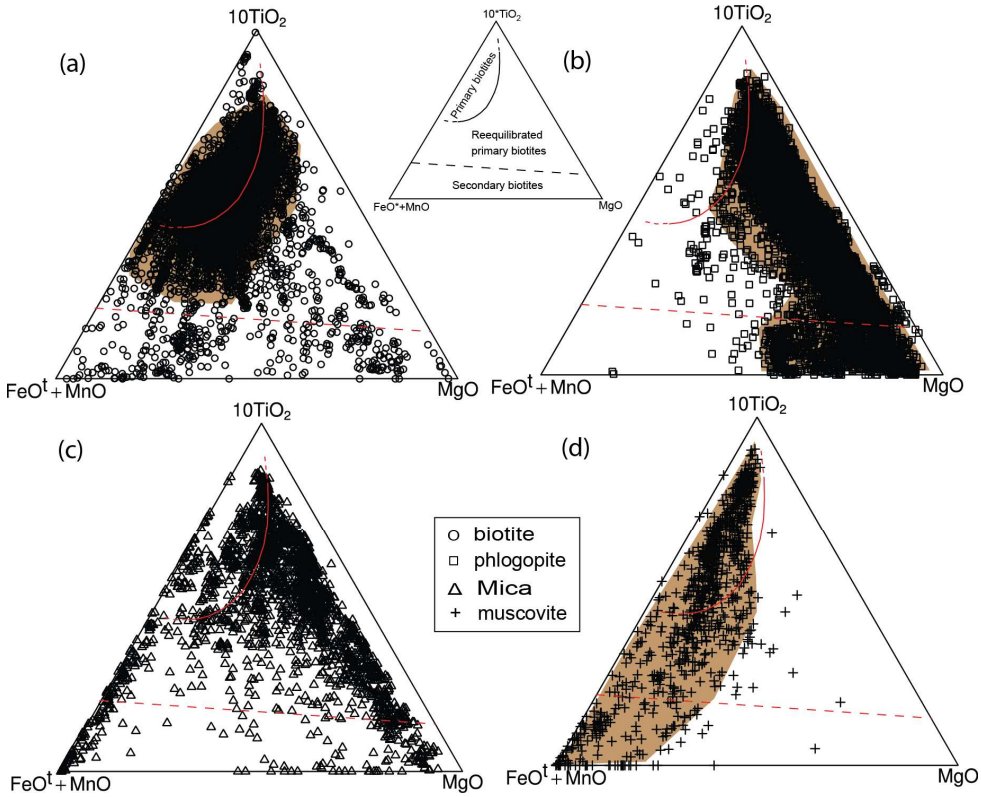

Figure 3. Ternary TiO_2–FeO+MnO–MgO diagram after Nachit et al. (2005); composition of biotite (a), phlogopite (b), Mica (c), and muscovite (d) from host-rocks of intra-plate setting. See the text for more details

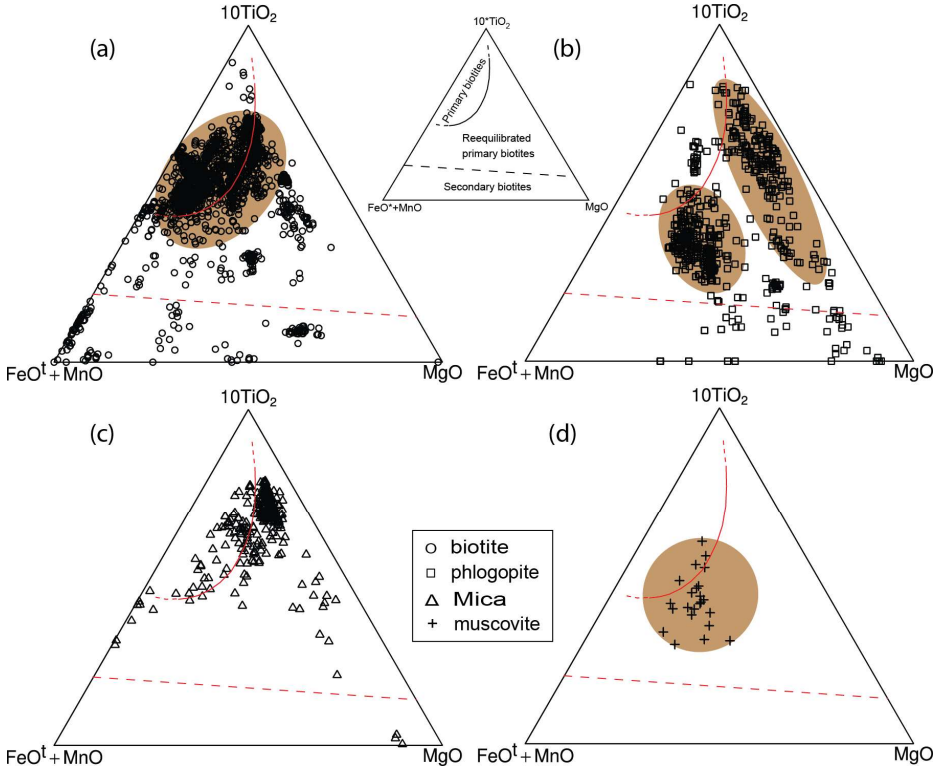

Figure 4. Ternary TiO_2–FeO+MnO–MgO diagram after Nachit et al. (2005); composition of biotite (a), phlogopite (b), Mica (c), and muscovite (d) from the rift setting. See the text for more details

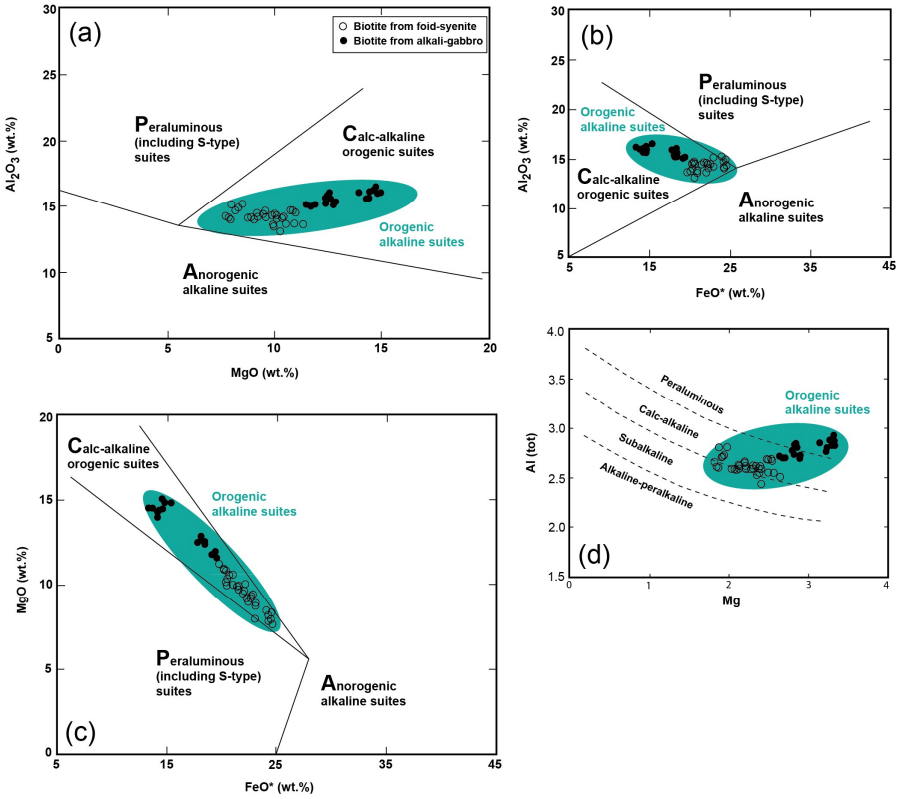

Figure 5. The chemical variation of biotite from subduction-related alkaline rocks and their plot in the calc-alkaline orogenic suites field (Ashrafi et al., 2009); diagrams of (a) MgO vs. Al_2O_3 (b) FeO^* vs. Al_2O_3 (c) FeO^* vs. MgO from Abdel-Rahman (1994) and (d) Mg vs. Al^{tot} from Nachit et al. (1985)

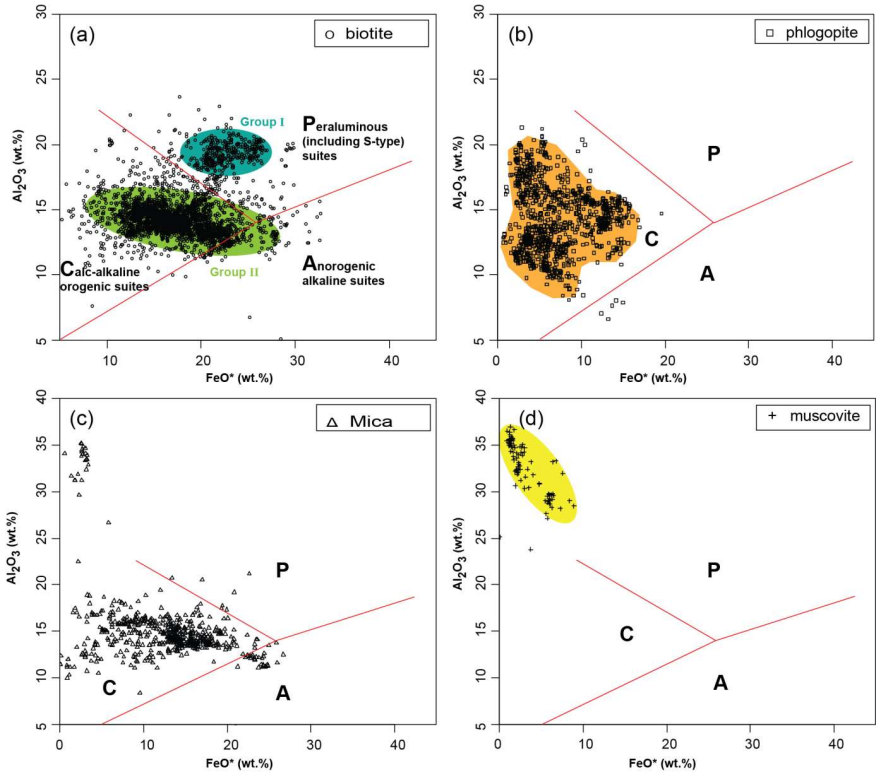

Figure 6. The composition of micas related to the convergent setting in FeO^t vs. Al_2O_3 variation diagrams; (a) biotite, (b) phlogopite, (c) Mica, and (d) muscovite. The red lines added to the diagrams, which separate the boundary of the A, C, and P fields, are from Abdel-Rahman (1994)

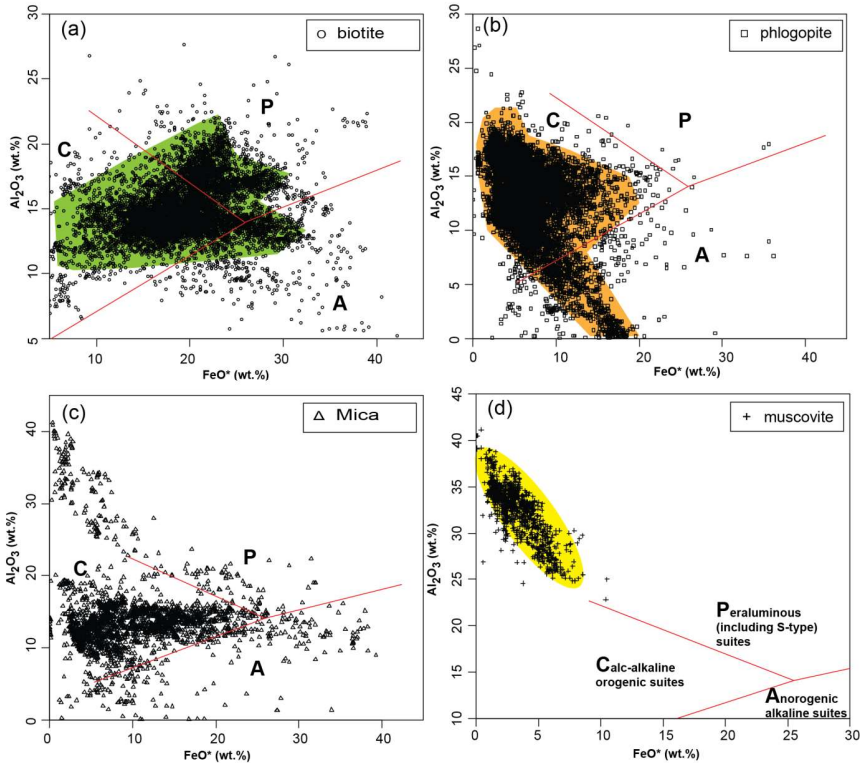

Figure 7. The composition of micas related to the intra-plate setting in FeO^t vs. Al_2O_3 variation diagrams; (a) biotite, (b) phlogopite, (c) Mica, and (d) muscovite. The red lines added to the diagrams, which separate the boundary of the A, C, and P fields, are from Abdel-Rahman (1994)

The FeO^t vs. Al_2O_3 variation plot for the rift setting micas indicates a significant scattering relative to the other settings (Figures 8a-d). Based on Figure 8b, the phlogopite data can be divided into two groups including Fe-rich and Fe-poor phlogopite. Similar to the previous diagrams, the muscovite data show a negative correlation (Figure 8d).

The MgO vs. Al_2O_3 variation plot shows that the biotites of convergent setting can be divided into two groups, equal to the calc-alkaline orogenic (C) and peraluminous (P) suites of Abdel-Rahman (1994)'s criteria (Figure 9a). The phlogopite compositions are plotted in the C field of Abdel-Rahman's classification with a shift towards high MgO contents (Figure 9b). Mica data mainly plot in the C field and do not show any correlation (Figure 9c). The muscovite compositions from the convergent setting show a negative correlation and are located in the upper part of the P field (Figure 9d).

The MgO vs. Al_2O_3 variation plot shows that the biotites of the intra-plate setting have a wide variation in MgO content (Figure 10a). In contrast, the phlogopite compositions show a broad variation in Al_2O_3 content (Figure 10b). Mica data mainly plot in the C field and do not show any correlation (Figure 10c).

These features show that regardless of the host rock type and mineral paragenesis, the composition of micas attributed to the intra-plate environment will lead to false results. The muscovite compositions from the intra-plate setting have a relative scattering in Al_2O_3 and MgO values (Figure 10d).

In the MgO vs. Al_2O_3 diagram for the biotites of the rift setting, there is much scatter in the data, and no particular trend can be considered; however, the data can be separated into several groups (Figure 11a). The phlogopite data can be divided into two groups rich in Mg and poor in Mg (Figure 11b). The data under the title "Mica" are scattered in such a way that they can be divided into three groups in terms of Al_2O_3 content (low, intermediate, and high in Al_2O_3) (Figure 11c).

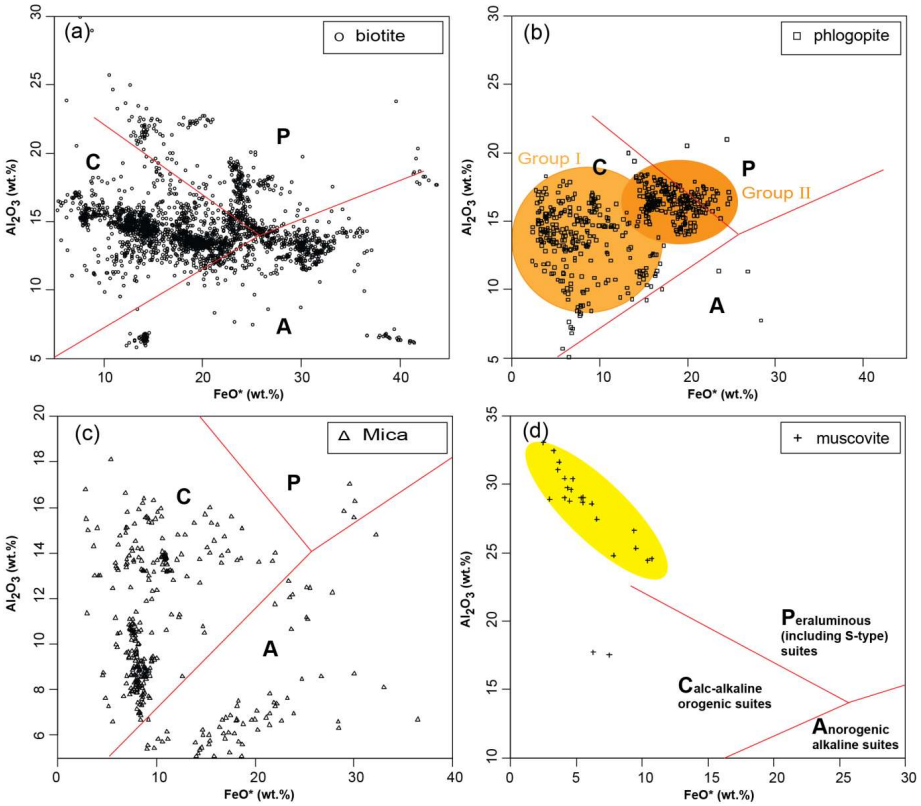

Figure 8. The composition of micas related to the rift setting in FeO^t vs. Al_2O_3 variation diagrams; (a) biotite, (b) phlogopite, (c) Mica, and (d) muscovite. The red lines added to the diagrams, which separate the boundary of the A, C, and P fields, are from Abdel-Rahman (1994)

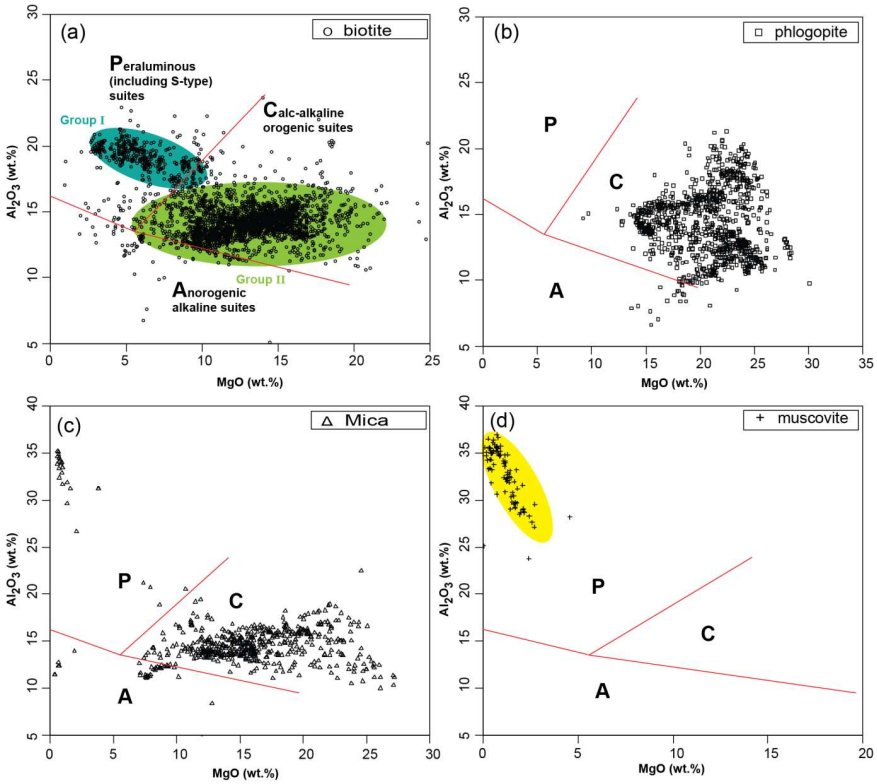

Figure 9. The composition of micas related to the convergent setting in MgO vs. Al_2O_3 variation diagrams; (a) biotite, (b) phlogopite, (c) Mica, and (d) muscovite. The red lines added to the diagrams, which separate the boundary of the A, C, and P fields, are from Abdel-Rahman (1994)

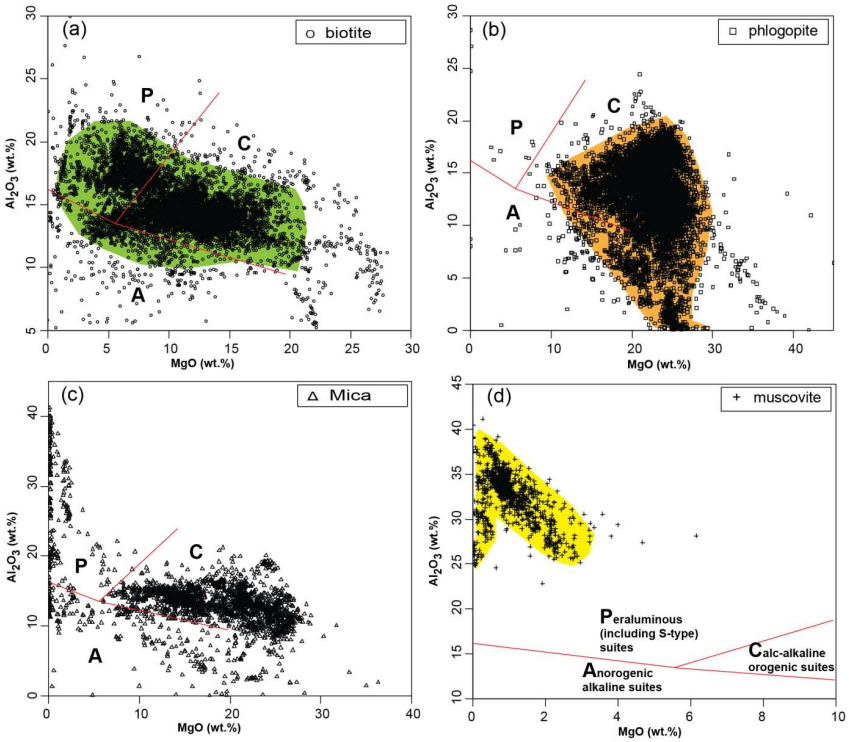

Figure 10. The composition of micas related to the intra-plate setting in MgO vs. Al_2O_3 variation diagrams; (a) biotite, (b) phlogopite, (c) Mica, and (d) muscovite. The red lines added to the diagrams, which separate the boundary of the A, C, and P fields, are from Abdel-Rahman (1994)

Almost a negative correlation between the two oxides is observed in the muscovite data (Figure 11d). There is a significant negative correlation between FeO^t and MgO in the biotite, phlogopite, and Mica of the convergent environment (Figures 12a-c).

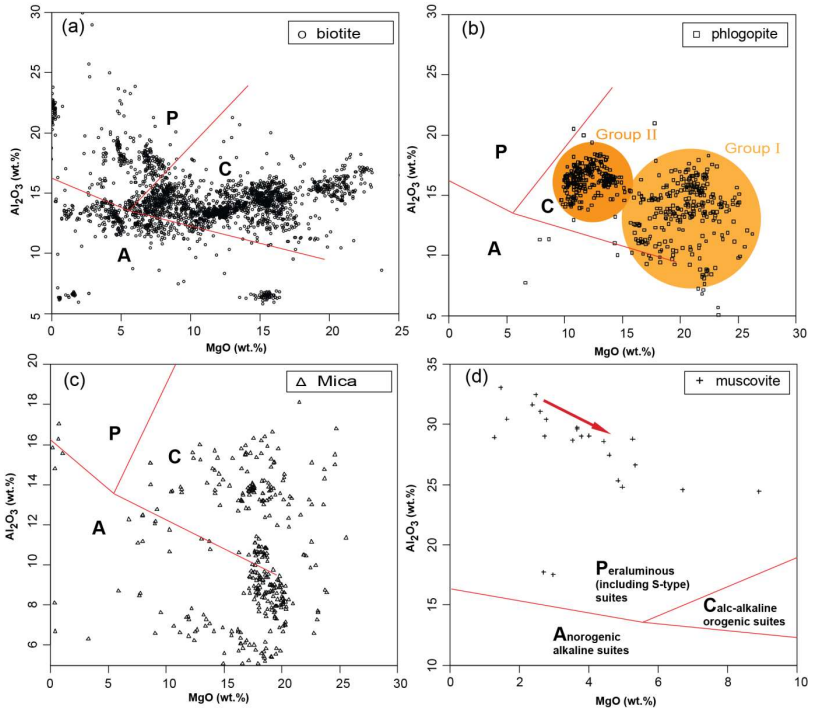

Figure 11. The composition of micas related to the rift setting in MgO vs. Al_2O_3 variation diagrams; (a) biotite, (b) phlogopite, (c) Mica, and (d) muscovite. The red lines added to the diagrams, which distinguish the boundary of the A, C, and P fields, are from Abdel-Rahman (1994)

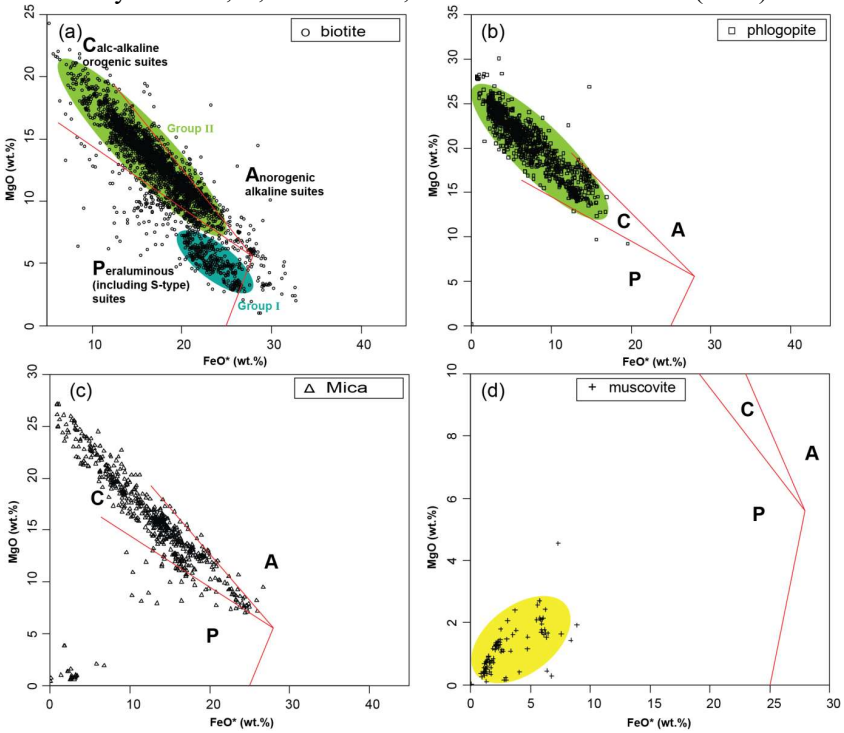

Figure 12. The composition of micas related to the convergent setting in FeO^t vs. MgO variation diagrams; (a) biotite, (b) phlogopite, (c) Mica, and (d) muscovite. The red lines added to the diagrams, which distinguish the boundary of the A, C, and P fields, are from Abdel-Rahman (1994)

Nevertheless, a positive correlation is visible for the muscovite between the two oxides (Figure 12d). These features can be seen for the micas of intra-plate and rift environments (Figures 13, 14).

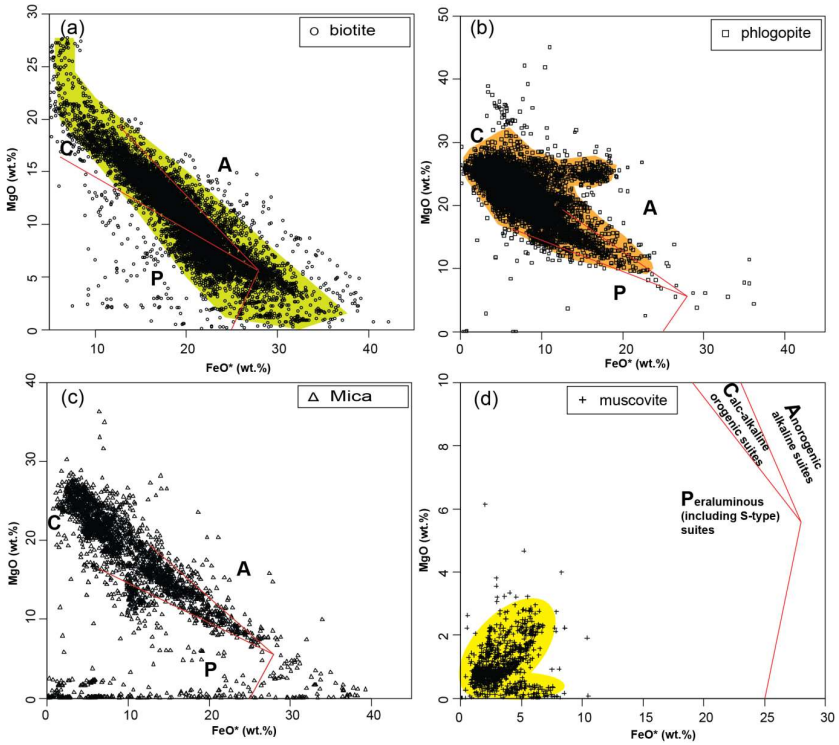

Figure 13. The composition of micas related to the intra-plate setting in FeO^t vs. MgO variation diagrams; (a) biotite, (b) phlogopite, (c) Mica, and (d) muscovite. The red lines added to the diagrams, which distinguish the boundary of the A, C, and P fields, are from Abdel-Rahman (1994)

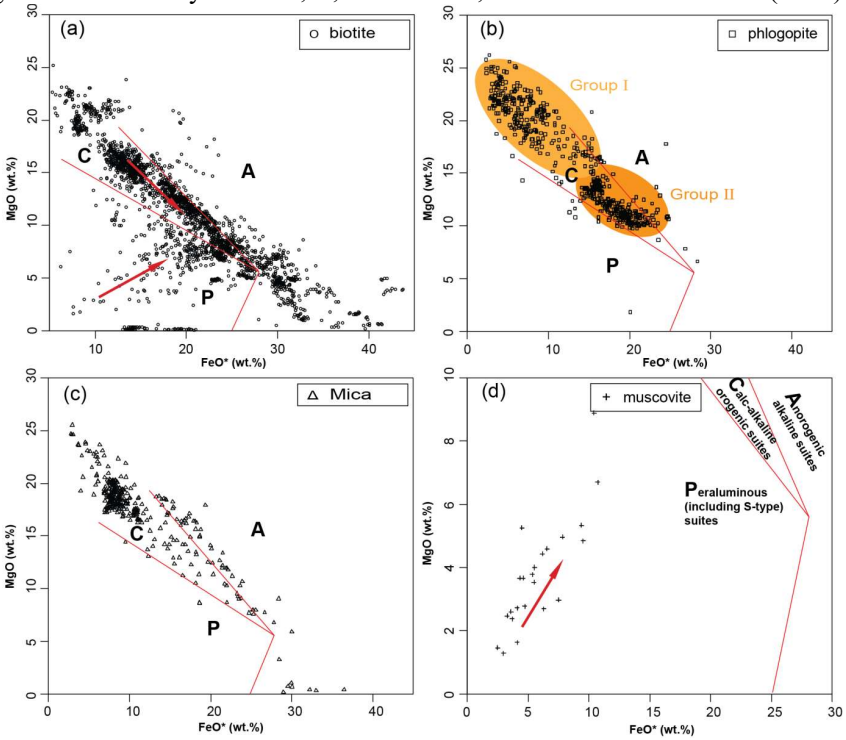

Figure 14. The composition of micas related to the rift setting in FeO^t vs. MgO variation diagrams; (a) biotite, (b) phlogopite, (c) Mica, and (d) muscovite. The red lines added to the diagrams, which distinguish the boundary of the A, C, and P fields, are from Abdel-Rahman (1994)

The range of variations in the amount of MgO is more at higher amounts of FeO^t; in other words, at higher amounts of iron, more scatter is seen in the trends (Figures 13a, b, d).

Based on the Al vs. Mg diagram, three groups or trends can be considered for the biotites of the convergent setting. As it is clear from the data distribution, unlike the three peraluminous, calc-alkaline, and sub-alkaline series, biotites belonging to the alkaline-peralkaline series are very rare (Figure 15a). Indeed, the phlogopite data will be plotted outside the range of the series specified for the biotites, due to their high Mg. However, if the dashed lines are extrapolated, the composition of phlogopites can be located within the range of each of the four series (Figure 15b). The Mica composition array in the diagram of Al vs. Mg is such that a negative or positive trend cannot be considered for it (Figure 15c). A negative correlation can be considered for the muscovite data (Figure 15d).

In general, the variation of biotite composition defines a negative Al-Mg correlation (Stussi & Cuney, 1996). This feature can be observed for the biotites of the intra-plate setting (Figure 16a). The most crucial feature of Figure 16b is the wide variation in the amount of Al^{tot} (apfu), which is revealed by the composition of phlogopite. The Mica composition, like the biotite, shows a negative correlation; however, the data has a considerable scattering (Figure 16c). Due to the high amounts of Al in the muscovite mineral, all the data of intra-plate muscovites are plotted in the peraluminous field. They show a negative correlation at higher amounts of Al. (Figure 16d).

The data related to the rift show a wide scatter, as shown in Figure 17; they can be divided into different groups (Figures 17a-c). For example, the phlogopite data can be divided into two groups of Mg-rich and Mg-poor (Figure 17b), and the Mica data can be divided into three groups of high, intermediate, and low Al (Figure 17c). This feature can be attributed to two factors, such as the incompleteness of the dataset or the presence of extreme differences in the host rock. The muscovite data has a negative correlation and has a peraluminous trend (Figure 17d).

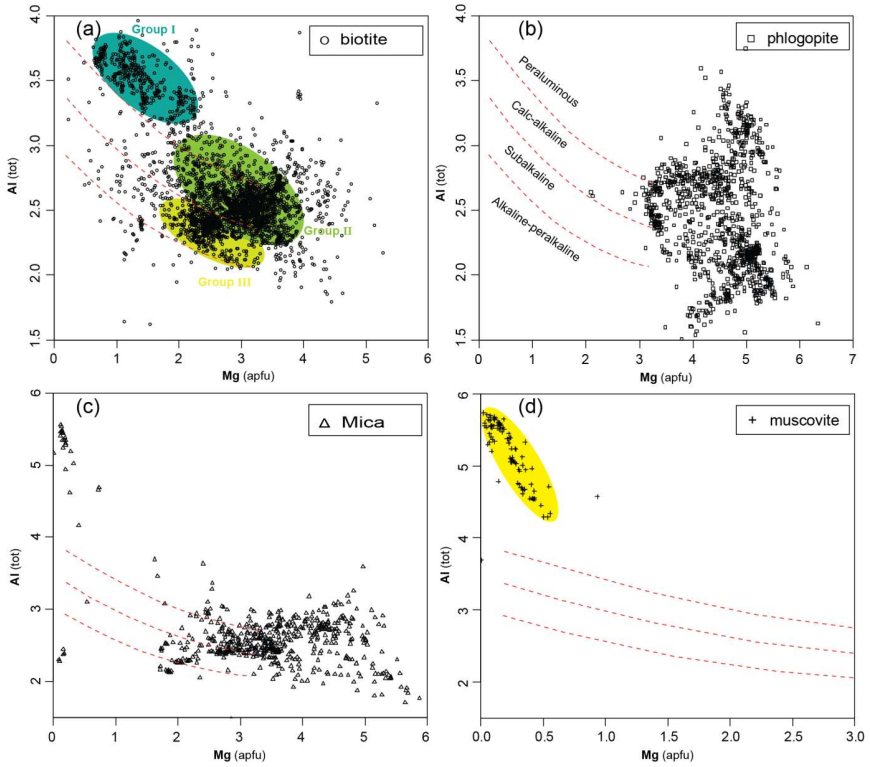

Figure 15. The Mg vs. Al variation diagrams for micas related to the convergent setting; (a) biotite, (b) phlogopite, (c) Mica, and (d) muscovite. The red dashed lines added to the diagrams, which distinguish the boundary of the peraluminous, calc-alkaline, subalkaline, and alkaline-peralkaline trends, are from Stussi & Cuney (1996)

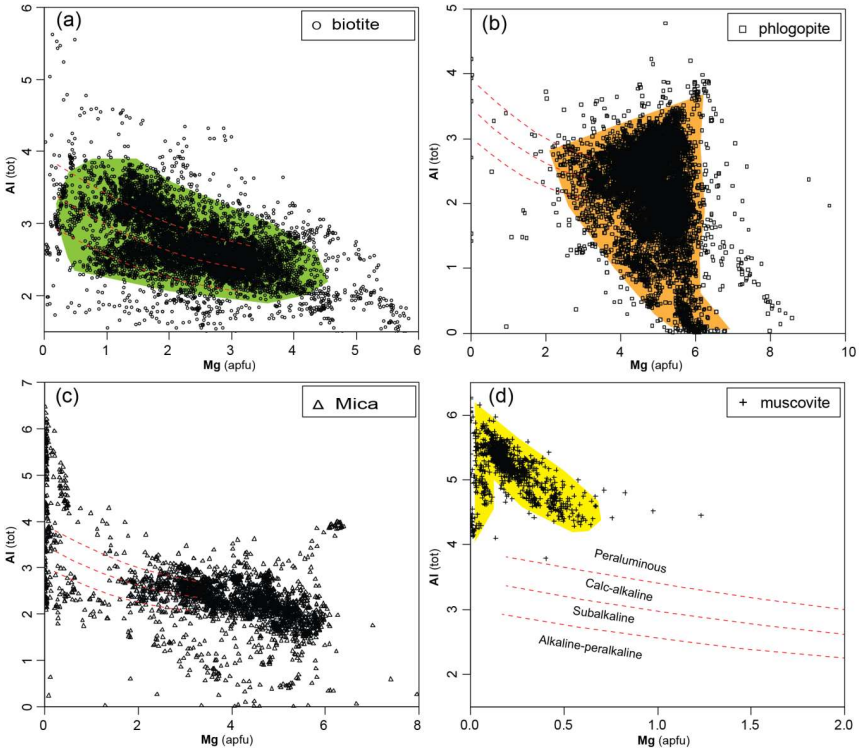

Figure 16. The Mg vs. Al variation diagrams for micas related to the intra-plate setting; (a) biotite, (b) phlogopite, (c) Mica, and (d) muscovite. The red dashed lines added to the diagrams, which distinguish the boundary of the peraluminous, calc-alkaline, subalkaline, and alkaline-peralkaline trends, are from Stussi & Cuney (1996)

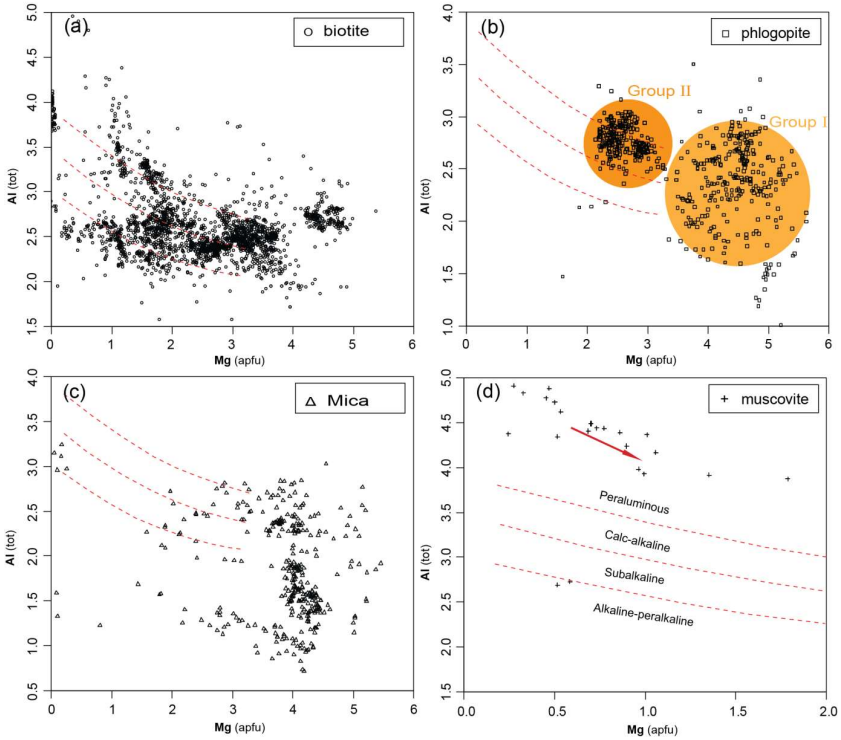

Figure 17. The Mg vs. Al variation diagrams for micas related to the rift setting; (a) biotite, (b) phlogopite, (c) Mica, and (d) muscovite. The red dashed lines added to the diagrams, which distinguish the boundary of the peraluminous, calc-alkaline, subalkaline, and alkaline-peralkaline trends, are from Stussi & Cuney (1996)

In the MgO-FeO^t-Al_2O_3 diagram (Figures 18-20; after Abdel-Rahman, 1994), most of the biotites of the convergent setting plot in the calc-alkaline orogenic suites (Figure 18a).

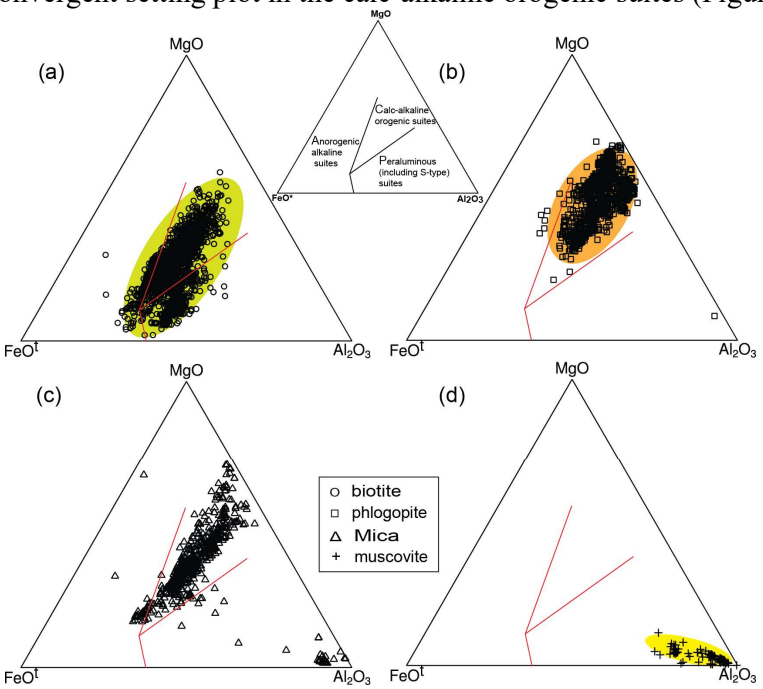

Figure 18. The ternary diagram of MgO-FeO^t-Al_2O_3 for comparison of the micas related to the convergent setting; (a) biotite, (b) phlogopite, (c) Mica, and (d) muscovite. The red dashed lines added to the diagrams, which distinguish the boundary of the peraluminous, calc-alkaline, and anorogenic alkaline trends, are after Abdel-Rahman (1994)

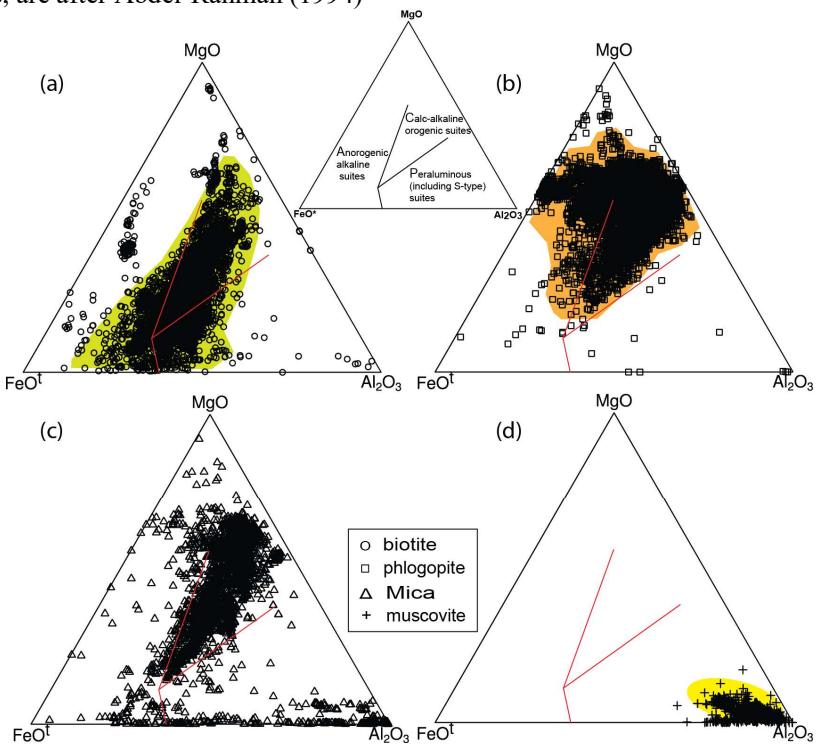

Figure 19. The ternary diagram of MgO-FeO^t-Al_2O_3 for comparison of the micas related to the intra-plate setting; (a) biotite, (b) phlogopite, (c) Mica, and (d) muscovite. The red dashed lines added to the diagrams, which distinguish the boundary of the peraluminous, calc-alkaline, and anorogenic alkaline trends, are after Abdel-Rahman (1994)

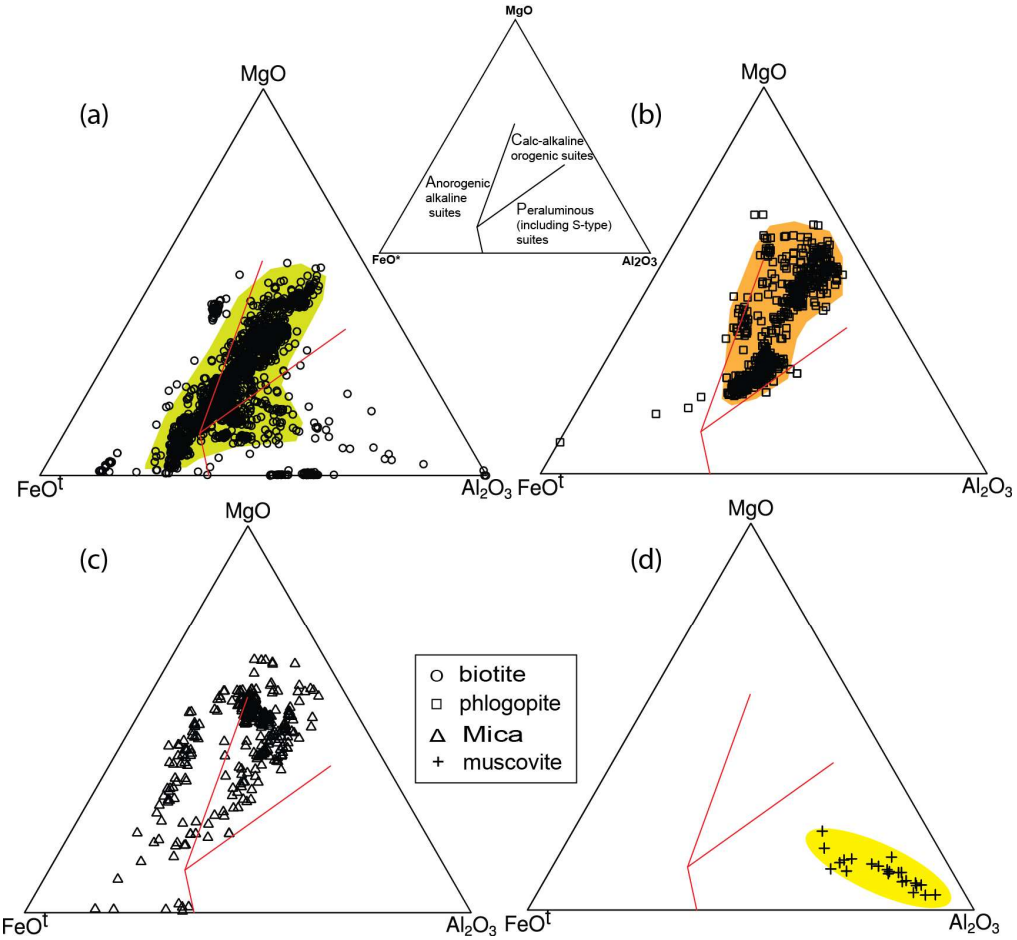

Figure 20. The ternary diagram of MgO-FeO^t-Al_2O_3 for comparison of the micas related to the rift setting; (a) biotite, (b) phlogopite, (c) Mica, and (d) muscovite. The red dashed lines added to the diagrams, which distinguish the boundary of the peraluminous, calc-alkaline, and anorogenic alkaline trends, are after Abdel-Rahman (1994)

The phlogopites of convergent environment are plotted in the same field. However, they are far from the intersection of the three fields specified by Abdel-Rahman (1994) (Figure 18b). The composition of phlogopites in the intra-plate environment is in the centre of the diagram, with a greater tendency towards the MgO corner (Figure 19b). In this diagram, the muscovite composition from all three tectonic environments is plotted near the Al_2O_3 corner (Figures 18d, 19d, and 20d). The biotite composition of the intra-plate environment is plotted around the junction of the three fields specified by Abdel-Rahman (Figure 19a). As to the Mica composition, the scattering of the data is remarkable, which could be since their type is not known (are they mostly biotite or phlogopite or muscovite or a combination of mica types?) (Figures 18c, 19c, and 20c).

Conclusions

The distribution of the data shows that biotites of the convergent environment can be divided into peraluminous with Mg-poor (Group I) and metaluminous with Mg-rich (Group II, III). This division can also be used for phlogopites of the rift environment, where Group I represents metaluminous (Mg-rich) phlogopites and Group II indicates peraluminous (Mg-poor) phlogopites. One of the most critical elemental substitutions in biotite and phlogopite is the substitution of Fe^{2+}=Mg^{2+}. Nevertheless, according to the occurrence of specific elemental

correlations, it seems that the substitutions of $3Mg^{2+}=2Al^{3+}$ and $3Fe^{2+}=2Al^{3+}$ in muscovite and $(Fe, Mg)^{2+}$ $Si^{4+}=$ ^{M}Al ^{T}Al in biotite and phlogopite are essential. Considering the various parameters involved in the composition of micas, their use to determine the magmatic suites and, thus, the tectonic environment must be combined with other findings. For example, the biotite compositions from orogenic alkaline suites plot in the C field of Abdel-Rahman's classification, therefore any composition that is plotted in this field can be related to alkaline or calc-alkaline orogenic suites. The amount of Mg in biotites of the convergent environment rarely reaches zero compared to the other two environments. The distribution of the data shows a relatively good negative correlation between Mg and Al^{tot} in biotites of intra-plate environment compared to phlogopites.

Acknowledgments

We are extremely grateful to the editors and reviewers of the journal, especially Dr A. Kananian and Dr A.A.T. Shabani for their valuable comments and efforts, which have helped to improve the manuscript. The authors also would like to acknowledge the GEOROC (Geochemistry of Rocks of Oceans and Continents) database and the references within it for providing the dataset.

References

Abdel-Rahman, A.F.M., 1994. Nature of biotites from alkaline, calc-alkaline, and peraluminous magmas. Journal of Petrology, 35: 525-541.

Abrecht, J., Hewitt, D.A., 1988. Experimental evidence on the substitution of tin in biotite. American Mineralogist, 73: 1275-1284.

Afshooni, S.Z., Mirnejad, H., Esmaeily, D., Asadiharoni, H., 2013. Mineral chemistry of hydrothermal biotite from the Kahang porphyry copper deposit (NE Isfahan), Central Province of Iran. Ore Geology Reviews, 54: 214-232.

Ashrafi, N., Jahangiri, A., Ameri, A., Hasebe, N., Eby, G.N., 2009. Biotite mineral chemistry of the Bozqush and Kaleybar alkaline igneous intrusions, NW Iran. Iranian Journal of Crystallography and Mineralogy, 17: 381-394 (in Persian with English abstract). http://ijcm.ir/article-1-568-fa.html

Ayati, F., Yavus, F., Noghreyan, M., Haroni, H.A., Yavuz, R., 2008. Chemical characteristics and composition of hydrothermal biotite from the Dalli porphyry copper prospect, Arak, central province of Iran. Mineralogy and Petrology, 94: 107-122.

Barbarin, B., 1990. Granitoids: Main petrogenetic classifications in relation to origin and tectonic setting. Geological Journal, 25: 227-238.

Boomeri, M., Mizuta, T., Ishiyama, D., Nakashima, K., 2006. Fluorine and chlorine in biotite from the Sarnowsar granitic rocks, northeastern Iran. Iranian Journal of Science and Technology, Transaction A30 (A1): 111-125.

Boomeri, M., Nakashima, K., Lentz, D.R., 2009. The Miduk porphyry Cu deposit, Kerman, Iran: a geochemical analysis of the potassic zone including halogen element systematic related to Cu mineralization processes. Journal of Geochemical Exploration, 103: 17-29.

Cottrell, E., Birner, S.K., Brounce, M., Davis, F.A., Waters, L.E., Kelley, K.A., 2021. Oxygen Fugacity Across Tectonic Settings. In: Moretti, R., Neuville, D.R. (Eds.), Magma Redox Geochemistry. American Geophysical Union, pp. 33-61. https://doi.org/10.1002/9781119473206.ch3

Deer, W.A., Howie, R.A., Zussman, J., 2013. An Introduction to the Rock Forming Mineral. Third Longman Editions, 498 pp.

Feng, Y., Deng, C., Xiao, B., Gong, L., Yin, R., Sun, D., 2021. Biotite geochemistry and its implication on the temporal and spatial difference of Cu and Mo mineralization at the Xiaokele porphyry Cu-Mo deposit, NE China. Ore Geology Reviews, 139: 104508. https://doi.org/10.1016/j.oregeorev.2021.104508

Foley, S.F., Prelevic, D., Rehfeldt, T., Jacob, D.E., 2013. Minor and trace elements in olivines as probes into early igneous and mantle melting processes. Earth and Planetary Science Letters, 363: 181-191.

Foster, M.D., 1960. Interpretation of the composition of lithium micas. US Geological Survey, 354: 11-49.

Heinrich, E.W., 1946. Studies in the mica group; the biotite-phlogopite series. American Journal of Science, 244(12): 836-848.

Huang, Y., Nakatani, T., Nakamura, M., Mccammon, C., 2019. Saline aqueous fluid circulation in mantle wedge inferred from olivine wetting properties. Nature Communications, 10: 1-10.

Janousek, V., Farrow, C.M., Erban, V., 2006. Interpretation of whole-rock geochemical data in igneous geochemistry: introducing Geochemical Data Toolkit (GCDkit). Journal of Petrology, 47: 1255-1259.

Kovalenko, V.I., Naumov, V.B., Girnis, A.V., Dorofeeva, V.A., Yarmolyuk, V.V., 2007. Average compositions of magmas and mantle sources of mid-ocean ridges and intraplate oceanic and continental settings estimated from the data on melt inclusions and quenched glasses of basalts. Petrology, 15(4): 335-368.

Liu, J.Q., Chen, L.H., Wang, X.J., Zhong, Y., Yu, X., Zeng, G., Erdmann, S., 2017. The role of melt-rock interaction in the formation of Quaternary high-MgO potassic basalt from the Greater Khingan Range, northeast China. Journal of Geophysical Research: Solid Earth, 122: 262-280.

Moshefi, P., Hosseinzadeh, M.R., Moayyed, M., Lentz, D.R., 2020. Distinctive geochemical features of biotite types from the subeconomic Sonajil porphyry-type Cu deposit, northwestern Iran: implications for analysis of porphyry copper deposit mineralization potential. Journal of Geochemical Exploration, 214: 106543.

Mullen, E.D., 1983. $MnO/TiO_2/P_2O_5$: A minor element discriminant for basaltic rocks of oceanic environments and its implications for petrogenesis. Earth and Planetary Science Letters, 62: 53-62.

Munoz, J.L., 1984. F-OH and Cl-OH exchange in mica with application to hydrothermal ore deposits. Reviews in Mineralogy, 13: 469-493.

Munoz, J.L., 1992. Calculation of HF and HCl fugacities from biotite compositions: revised equations. Geological Society of America Abstracts with Programs, 24: p. 221.

Nachit, H., Ibhi, A., Abia, E.H., Ohoud, M.B., 2005. Discrimination between primary magmatic biotites, reequilibrated biotites and neoformed biotites. Comptes Rendus Geoscience, 337: 1415-1420.

Nachit, H., Razafimahefa, N., Stussi, J.M., Caron, J.P., 1985. Composition chimique des biotites et typologie magmatique des granitoïdes. Comptes rendus hebdomadaires des séances de l'Académie des sciences, 301: 813-818.

Patiño Douce, A.E., 1993. Titanium substitution in biotite: an empirical model with applications to thermometry, O_2 and H_2O barometries, and consequences for biotite stability. Chemical Geology, 108: 133-162.

Rieder, M., Cavazzini, G., D'Yakonov, Y.S., Frank-Kamenetskii, V.A., Gottardi, G., Guoggenheim, S., Koval, P.V., Muller, G., Neiva, A.M.R., Radoslovich, E.W., Robert, J.L., Sassi, F.P., Takeda, H., Weiss, Z., Wones, D.R., 1998. Nomenclature of the micas. Canadian Mineralogist, 36: 41-48.

Saha, R., Upadhyay, D., Mishra, B., 2021. Discriminating tectonic setting of igneous rocks using biotite major element chemistry−A Machine Learning Approach. Geochemistry, Geophysics, Geosystems, 22(11): e2021GC010053 https://doi.org/10.1029/2021GC010053

Samadi, R., Torabi, G., Kawabata, H., Miller, N.R., 2021. Biotite as a petrogenetic discriminator: Chemical insights from igneous, meta-igneous and meta-sedimentary rocks in Iran. Lithos 386-387, 106016.

Schmidt, M.W., Jagoutz, O., 2017. The global systematics of primitive arc melts. Geochemistry, Geophysics, Geosystems, 18: 2817-2854

Shabani, A.A.T., Lalonde, A.E., Whalen, J.B., 2003. Composition of biotite from granitic rocks of the Canadian Appalachian orogen: A potential tectonomagmatic indicator? Canadian Mineralogist, 41(6): 1381-1396.

Stussi, J.M., Cuney, M., 1996. Nature of biotites from alkaline, calc-alkaline and peraluminous magmas by Abdel-Fattah M. Abdel-Rahman: a comment. Journal of Petrology, 37: 1025-1029.

Ueki, K., Iwamori, H., 2014. Thermodynamic calculations of the polybaric melting phase relations of spinel lherzolite. Geochemistry, Geophysics, Geosystems, 15: 5015-5033.

Van Middelaar, W.T., Keith, J.D., 1990. Mica chemistry as an indicator of oxygen and halogen fugacities in the Can Tung and other W-related granitoids in the North American Cordillera. In: Stein, H.J., Hannah, J.L. (Eds.), Ore-bearing Granite Systems; Petrogenesis and Mineralizing

Process. Geological Society of America, Special Paper 246: 205-220.
Wones, D.R., Eugster, H.P., 1965. Stability of biotite: Experiment, theory, and application. American Mineralogist, 50: 1228-1272.
Zhang, W., Lentz, D.R., Thorne, K.G., McFarlane, C., 2016. Geochemical characteristics of biotite from felsic intrusive rocks around the Sisson Brook W-Mo-Cu deposit, west central New Brunswick: an indicator of halogen and oxygen fugacity of magmatic systems. Ore Geology Reviews, 77: 82-96.